Thermodynamic activity measurements of iron in Fe-Zr alloys by high temperature mass spectrometry

Sylvie Chatain, Bruno Larousse, Claude Maillault, C. Gueneau, Christian Chatillon

Thermodynamic activity measurements of iron in Fe-Zr alloys by high temperature mass spectrometry

S. Chatain°, B. Larousse°, C. Maillault°, C. Guéneau° and C. Chatillon*,

° Commissariat à l'Energie Atomique Saclay, Direction de l'Energie Nucléaire / Division des Activités Nucléaires de Saclay / Département de Physico-Chimie / Service de Chimie Physique / Laboratoire de Modélisation, de Thermodynamique et de Thermochimie, 91191 Gif-sur-Yvette Cedex, France

* Laboratoire de Thermodynamique et Physico-Chimie Métallurgiques (CNRS UMR 5614, UJF/INPG), ENSEEG – Domaine Universitaire, BP 75, 38402 Saint Martin d'Hères Cedex, France

Abstract

The thermodynamic activity of Fe in the Fe-Zr alloys respectively for the temperature and composition ranges of T= 1501 K – 1852 K and x_{Zr} = 50 to 95 at.%, has been measured by the multiple Knudsen effusion cell – mass spectrometric method. The liquidus temperature of the three compositions 55, 60 and 85 Zr at. % are determined from the variations of activity and compared with the literature data.

I- Introduction

The iron-zirconium system is an important basic chemical system for nuclear material applications for both low and high temperature ranges. The low temperature application is related to the behaviour of cladding tube study in Pressurized Water Reactor. Two industrial alloys are commonly used, Zircaloy-4 with Sn, Fe, Cr and O as additive elements and M-5^{TM} with Nb, Fe

and O. Iron has a low solubility in α-Zr (hcp) (low temperature phase) and then intermetallic phases Fe_xZr_y precipitate. This feature changes the corrosion behaviour and the chemical properties of the cladding tubes. The thermodynamic knowledge of the Zr-Fe-Sn-Nb-O quinary system is needed in order to predict which kind of intermetallic phase can precipitate [1].

For the high temperature application, Fe-Zr binary is part of the U-Zr-O-Fe quaternary system which is a key system for in-vessel corium studies. Corium is the mixture resulting from the hypothetical partial or complete melting of reactor assembly mainly constituted of zircaloy sheaths, UO_2 fuel pellets and iron is representative of the steel vessel. The heat transfer processes occurring in corium can be predicted when the natures and relative fractions of liquid and solid phases are known as a function of temperature and composition [2].

The Fe-Zr binary is definitely the sub-system common base for the description of the two materials behaviour and it is necessary to have a good thermodynamic knowledge of the basic binaries and ternaries to well describe quaternary and higher order systems.

The Fe-Zr system has been quite extensively studied in the past. The critical evaluation of the system has been performed by Arias et al. [3-4], Alekseeva et al. [5] and Okamoto [6]. Thermodynamic modellings by the CALPHAD method have been performed by Pelton [7], Servant et al [8] and recently by Jiang et al. [9]. In 2002, Stein et al. [10] studied experimentally the whole phase diagram by using differential thermal analysis (DTA), electron-probe microanalysis (EPMA), X-ray diffraction (XRD), and metallography. These last authors reported a new phase diagram with the following and new main features. The $Fe_{23}Zr_6$ compound is not an equilibrium phase of the only binary system but an oxygen-stabilized phase since it always occurs only as a third phase containing up to 1 wt.% O added to the observed (α-Fe) and Fe_2Zr phases in the heat-treated binary alloys. The Laves phase Fe_2Zr has a cubic crystalline structure

(C15) at the stoechiometric composition and a hexagonal C36-type polymorph structure at high temperature with Zr concentrations as low as 26.6 at.%. $FeZr_2$ is a high temperature phase, stable only between 1053 and 1224 K.

Concerning the high temperature experimental data, we observe first that the liquid thermodynamic data are sparse and second that there is a large uncertainty about the shape of the liquidus curve due to lack of consistent data.

The mixing enthalpies of the liquid phase were derived from calorimetric measurements by Sudatsova et al. [11], Sidorov et al. [12] and Wang et al. [13]. The values of Sidorov et al. differ notably from the other two sets of measurements. Schindlorova and Buzek [14] calculated the activities of Fe and Zr by means of a thermodynamic analysis of the phase diagram at 1873K in the composition range between 13 and 79 at. %.

In the Fe_2Zr-Zr area, the only liquidus temperature measurements of Svechnicov [15], Stein [10] and Servant [8] are available (Table 1).

Since no direct activity measurements in the liquid phase are available, we have undertaken the present high temperature investigation by High Temperature Mass Spectrometry using a multiple Knudsen cell coupled to a quadrupole mass spectrometer.

II- Experimental method

Multiple Knudsen cell mass spectrometry is now a standard method for studying chemical equilibria at high temperature [16,17,18]. Our apparatus has already been described by Gardie et al. [19] and then by Baïchi et al. [20] who improved the method with a restricted collimation device in order to discard the detection of parasitic surface re-vaporizations [21]. The envelope of the four effusion cells was made of molybdenum and the four Knudsen cells (crucible and lid)

were made of pure ceramic oxide, hypostoechiometric yttria, Y_2O_{3-x} for the alloys or dense alumina : Al_2O_3 for the reference (pure Fe). Y_2O_{3-x} exhibited a low chemical reactivity with regard to Fe-Zr liquid alloys. Our device and the Knudsen cell geometry are shown in ref [21]. The temperature is measured with a W-Re thermocouple calibrated in situ on the gold and iron melting points as observed by mass spectrometry monitoring of ionic intensities, with an accuracy of ± 5 K.

In our experimental conditions, the gaseous phase is in equilibrium with the condensed phase. This vapour phase is rarefied and can be considered as ideal. The thermodynamic activity a_i of the component *i* of the mixture Fe-Zr can be defined as the ratio of the partial vapour pressure p_i^m of component *i* over the mixture to the vapour pressure p_i^0 of the pure element, at the same temperature. The mass spectrometer allows us to measure the ionic intensity of component *i* which yields the partial pressure $p_i=I_iT/S_i$. With our restricted collimation device, the sensitivity S_i relative to component *i* remains constant whatever the cell considered [22] and consequently, the activity equals the ratio of the ionic currents of *i* measured over the mixture and over the pure element :

$$a_i=\frac{p_i^m}{p_i^0}\cong\frac{I_i^m}{I_i^0} \qquad (1)$$

Ten samples with nominal Zr contents of 50, 55, 60, 67, 71, 75, 78, 85, 90 and 95 at. % were elaborated at CEA Saclay (DRT/S3ME/LTMEX) from pure Fe (99.9 % Optilas) and Zr (Van Arkel with 27 ppm of oxygen) by arc melting under an argon atmosphere in a water-cooled copper crucible. For each as cast alloy, the iron and zirconium contents were analyzed by ICP-AES and the oxygen content by reduction melting and infra-red absorption. The resulting compositions are presented in table 2. We observe an upper oxygen content for high iron content.

Our technique requires the beam to be in the molecular flow regime, which correspond to a pressure in the cell < 10^{-4} bar, and the vapour pressures of the components have to be high enough to yield measurable ion currents. Iron is much more volatile than zirconium (at T=1773 K, $p^{\circ}_{(Fe)}$ = 1.89 Pa and $p^{\circ}_{(Zr)}$ = 4.6×10^{-6} Pa [22]) and thus, in the temperature range defined by iron pressures, it was not possible to measure simultaneously the ionic current of Zr and Fe and consequently to obtain simultaneously the two activities. The activity determinations of Fe were performed using a pure Fe reference and the main mass peak i.e ^{56}Fe (91.8 %) was measured at 15 eV ionizing energy.

We have checked the precision of the micrometric movement for automatic adjustment of the position under vacuum with an alumina crucible containing an iron sample at temperature of about 1739 K. No appreciable clearance was detected when we approached the same orifice position in both X and Y-direction (Fig. 1) and a plateau is also observed as already analyzed by M. Heyrman et al [22].

We also performed an experiment to test the isothermal nature of the effusion cells in the multiple cell device. Four alumina effusion cells filled with pure iron sample (about 2-3 g) were placed in the multiple cell envelop. At the iron melting point, the ion intensity ratios differed by less than 4% (included thermal and position uncertainties) (Fig.2).

During each investigation, we checked that there was no significant shift of the mass spectrometer sensitivity by monitoring the I.T logarithm versus the inverse of temperature. Moreover, we recorded the intensity with increasing temperature then decreasing temperature. We finally checked the reproducibility at a given temperature (Fig. 3). The difference did not exceed 3 %. Furthermore, the iron content of alloys was analyzed after each experiment and the composition evolution due to preferential loss by effusion of Fe did not exceed 2%.

III- Iron activity results

The thermodynamic activities of Fe in the Fe-Zr system were measured for in the x_{Zr}=50 to 95 at.% and 1501 K to 1852 K temperature ranges with pure solid or liquid iron as a reference. Our field of investigation, as shown in Fig. 4, included liquid alloys and several two-phase regions, liquid+Fe_2Zr and liquid+β-Zr. Experimental ln(a_{Fe}) data referred to pure iron are presented in Fig. 5 versus $10^4/T(K^{-1})$. Activity values are referred to γ-solid iron for T<1667 K, to the δ-solid iron in the 1678-1811 K temperature range and to the liquid iron for T>1811 K. A few measurements have been performed relative to pure liquid iron, but we have not observed any significant change in the slope of the activity curves since the temperature range (1811- 1852 K) is quite small. Due to the low value of $\Delta H^0_{Fe}(\gamma \rightarrow \delta)$ = 836 J.mol^{-1} [23], the activities referred to γ or δ-solid pure iron are not significantly different. The activity depends only on the temperature in the two-phase region since the variance equals unity and on temperature and composition within the divariant liquid region. We observed a slope change on the activity curves for 55, 60 and 85 Zr at. % contents which corresponds to the liquidus transition (liquid+$Fe_2Zr \rightarrow$ liquid) or (liquid+β-Zr $\rightarrow$ liquid). Calculation of the intersept gives the liquidus temperatures that are presented in Table 1.

For each area, a linear least-mean-square fit is performed as : $\ln(a_{Fe}) = (A \pm \delta A) + (B \pm \delta B) / T$ (Tables 3 and 4). The average standard deviations in the slope B and the constant coefficient A are calculated using the statistical formulae proposed by Paule and Mandel [24].

IV- Analysis and discussion

IV.1- Molar excess functions of liquid Fe, Zr and alloy

In the following, we derive an expression for the partial molar excess Gibbs energy of iron in the Fe-Zr liquid alloy from our activity measurements,. To refer a liquid alloy to liquid elements, the reference state change is calculated according to ref. [18] :

$$\ln\frac{a^{s}_{Fe}}{a^{l}_{Fe}}=\frac{\Delta H^{0}_{m(Fe)}}{RT}.\frac{T_{m(Fe)}-T}{T_{m(Fe)}} \qquad (2)$$

where a^{l}_{Fe} denotes the activity referred to the pure undercooled liquid iron, a^{s}_{Fe} the activity referred to the pure solid iron, $\Delta H^{0}_{m(Fe)}$ and $T_{m(Fe)}$ the iron melting enthalpy and temperature which are chosen from Pankratz [25] : $\Delta H_{m(Fe)}$ = 13.794 kJ.mol^{-1}, $T_{m(Fe)}$ = 1811 K.

In order to determine a general relation for the partial molar excess Gibbs energies, the following α_i-functions [26] are used :

$$\alpha_i=\frac{\Delta\overline{G}_i^{xs}}{(1-x_i)^2}=\frac{RT\ln(a_i/x_i)}{(1-x_i)^2} \qquad (3)$$

that we fitted with a polynomial expression of the minimum degree. In the case of iron, it is sufficiently accurate to use a linear fit as shown at 1700 K in Fig. 6

$$\alpha_{Fe}=A(T)+B(T)(1-x_{Fe}). \qquad (4)$$

The computed coefficients A and B are linear versus temperature.

The zirconium activity can be calculated by integration of the Gibbs-Duhem relation :

$$\sum x_i d\ln(a_i)=0. \qquad (5)$$

The Gibbs-Duhem's equation yields

$$\alpha_{Zr}=C(T)+D(T)(1-x_{Zr}) \qquad (6)$$

where

$C(T)=A(T) + (3/2)B(T)$

$D(T)=-B(T)$.

From equations (4) and (6), the molar excess Gibbs energy of the (Fe, Zr) liquid alloys referred to the liquid elements (in Joule per mole) can be deduced :

$$\Delta G^{xs}(L)=x_{Fe}x_{Zr}\left[E(T)+F(T)\left(x_{Fe}-x_{Zr}\right)\right] \qquad (7)$$

where

$E(T)=A(T) + (3/4)B(T)$

$F(T)=-B(T)/4$.

The values of the partial molar excess Gibbs energy parameters are listed in Table 5.

IV.2- Comparison of our activity results with literature

The iron activity referred to liquid Fe and zirconium activity referred to liquid Zr can be deduced respectively from equations (4) and (6). In the following, we compare our results with the data published in the literature (Fig. 7). Schindlorova and Buzek [14] calculated the activities of Fe ans Zr at 1873 K in the composition range 13-79 at.% Zr. The values were established by means of a thermodynamic analysis of the Fe-Zr phase diagram. Pelton deduced the properties of the liquid phase from one point on the iron-liquidus curve, the eutectic point at 8.8 at.% Zr at T=1608 K and one point on the zirconium-liquidus curve, the eutectic point at 76 at.% Zr at T=1201 K [7]. Moreover, the liquidus was optimised as a sub-regular solution with excess entropy, ΔS^{xs}, and excess enthalpy, ΔH^{xs}, given by

$\Delta S^{xs}(L) = 0$

$$\Delta H^{xs}(L) = x_{Fe}\, x_{Zr}\, (-66\,948 - 29\,050 x_{Zr}) \qquad (8).$$

We can thus calculate the Fe and Zr activity referred to the pure liquid component from the equation (8) as $\Delta G^{xs}(L) = \Delta H^{xs}(L)$ and $\Delta\overline{G}_i^{xs} = \frac{\partial \Delta G^{xs}}{\partial N_i} = RT\ln\left(a_i / x_i\right)$, where N_i is the mole number of component i.

We note that our experimental results differ from the activities deduced from Schindlorova et al. and Pelton models which are in good agreement with each other. This discrepancy is larger for zirconium for which no measurement was performed.

The activity of Fe and Zr presents a strong negative deviation from Raoult's law which corresponds to a strong attractive potential of the component in the liquid phase.

IV.3- Gibbs energy formation of Fe_2Zr

The expressions for ΔG_{Fe}^{xs} and ΔG_{Zr}^{xs} also yield some thermodynamic properties of the compounds. Using relations (4) and (6), the boundaries of the phase diagram and the properties of pure Fe and Zr, we deduced the free enthalpy of formation of the Fe_2Zr intermetallic compound.

The free enthalpy of formation of Fe_2Zr corresponds to the reaction :

$$2\,Fe_{(s)} + Zr_{(s)} \leftrightarrow Fe_2Zr_{(s)} \qquad (9)$$

On the liquidus curve, as 1224 K < T < 1946 K, the following equation takes place

$$2Fe_{(l)} + Zr_{(l)} \leftrightarrow Fe_2Zr_{(s)} \qquad (10)$$

with the following Gibbs energy : $\Delta G_f^0(Fe_2Zr) = -RT\ln(a_{Zr} \cdot a_{Fe}^2)$.

Free energy referred to the solid elements (equilibrium (9)), is calculated from melting Gibbs energy of Fe and Zr at each temperatures using : $\Delta G_{ref\ liq} = \Delta G_{ref\ sol} + 2\Delta G_{m\ (Fe)} + \Delta G_{m(Zr)}$ with

$\Delta G_{m\ (Fe)}$ = 13807 – 7.632T and $\Delta G_{m(Zr)}$ = 9656.7 + 68.927T + 23.221.$10^{-4}T^2$ – 10.234TlnT in J/mol and T in K [27].

In Table 6, we compare our values of free energies of formation with those evaluated by Pelton [7] from

i) the enthalpy of formation of Fe_2Zr from solid elements measured calorimetrically at 1487 °C by Gachon and Hertz [28]

ii) the change to the liquid standard state with the Gibbs energies of melting $\Delta G_{m\ (Fe)}$, $\Delta G_{m(Zr)}$.

iii) the melting point at 1675°C.

The result in joules per mole of atoms is

$$\Delta G_f^0\left(Fe_2Zr\right) = -46442 + 9.8073T \qquad (12).$$

Our values are in quite good agreement with those of Pelton. We note that the agreement is better for the low temperatures than for the higher ones. At first, no activity data has been measured in this part of the phase diagram, so the activity data used for our calculation are extrapolated from the relation (4) both in temperature and composition. Then, the liquidus composition is estimated from Stein's phase diagram which is different from the Pelton's one.

V- Conclusion

The thermodynamic activities of Fe in the Fe-Zr alloys for the temperature and composition range T= 1501 K – 1852 K and X_{Zr} = 50 to 95 at.%, have been measured by multiple Knudsen effusion cell – mass spectrometry method. From the $\ln(a_{Fe}) = f(10^4/T)$ linear fits of experimental data, the partial molar excess Gibbs energies of Fe and Zr referred to the pure liquid elements are calculated with a polynomial fit of the third degree. The liquidus temperatures of three

compositions 55, 60 and 85 Zr at. % are determined from the variations of activities. The liquidus temperatures are in quite good agreement with phase diagram proposed by Stein.

Acknowledgments

The authors would like to thanks P. Olier (DRT/DTEN), M. Tabarant, V. Delanne and V. Dauvois (DEN/DPC) for their help in the elaboration of alloys, for ICP-AES analysis of iron and zirconium and the oxygen content by reduction melting – infra-red absorption analysis.

Nominal Composition of the sample (at.% Zr)	Measured Composition for the samples (at.% Zr)	Liquidus Temperature (°C)	Reference
60	64.7	1349*	[10]
80	79.9	1364	[10]
80	81	1442	[10]
67		1297	[8]
74		950	[15]
55	56.1 ± 3.8	1347±30	this work
60	60.2 ± 3.0	1291±30	this work
85	87.2 ± 3.6	1408±15	this work

Table 1. Experimental values of the liquidus temperatures in the Fe_2Zr-Zr area.

Nominal Composition (at . % Zr)	Measured Composition (at. % Zr)	Measured Composition (at. % Fe)	Oxygen Content (% at. O)
50	19.5-60.0	40.0-80.35	0.149-0.192
55	47.6-52.4	47.3-52.1	0.272-0.278
60	57.4-63.4-	36.4-42.4	0.185-0.19
67	32.1-32.4	67.5-67.8	0.11-0.12
71	72.2	27.6	0.14
75	74.2	25.7	0.05
78	78.3	21.6	0.03
85	83.6	16.4	0.03
90	89.4	10.5	0.06
95	94.8	5.1	0.05

Table 2. Compositions range of our as cast alloys and their oxygen content deduced from two different samples analysis.

X_{Zr} (at. %)	$\ln(a_{Fe}) = (A \pm \delta A) + (B \pm \delta B)/T$	temperature range (K)
87.2	-(0.4929 ± 0.3399) - (6347 ± 588) / T	1677-1807
80.4	-(1.1732 ± 0.2433) - (4058 ± 411) / T	1563-1809
74.4	-(0.8384 ± 0.1705) - (4116 ± 289) / T	1530-1809
73.3	-(1.0274 ± 0.1373) - (3419 ± 232) / T	1563-1809
68.0	-(1.2648 ± 0.3322) - (2791 ± 581) / T	1563-1787
60.2	-(0.2901 ± 0.2141) - (3324 ± 364) / T	1583-1807
56.1	(0.1320 ± 0.4078) - (3751 ± 702) / T	1615-1807

Table 3. Natural logarithms of iron activity in our liquid alloys fitted as $\ln(a_{Fe})=A+B/T$ with respect to pure solid Fe as reference.

Two-phase area	$\ln(a_{Fe}) = A + B/T$
Liquid + β- Zr	-(5.9677 ± 0.2088) + (2854 ± 360) / T
Liquid + Fe_2Zr	(4.2580 ± 0.2072) – (10 437 ± 334) / T

Table 4. Natural logarithms of our iron activity for the two-phase field alloys fitted as $\ln(a_{Fe})=A+B/T$ with respect to pure solid Fe as reference.

Iron	Zirconium	Liquid
A(T) = - 221 264 + 77.221T	C(T) = 44 511 – 29.752T	E(T) = - 88 377 + 23.735T
B(T) = 177 183 – 71.315T	D(T) = - 177 183 + 71.315T	F(T) = - 44 296 + 17.829T

Table 5 Partial molar excess Gibbs energy parameters (in joule per mole) for the (Fe, Zr) alloys referred to liquid elements

T (K)	X_{Zr} liquidus (deduced from Stein's phase diagram) (at. %)	$\Delta_f G^0(Fe_2Zr)$ (kJ mol^{-1}) liquid reference (this work)	$\Delta_f G^0(Fe_2Zr)$ (kJ mol^{-1}) liquid reference Pelton [7]	$\Delta_f G^0(Fe_2Zr)$ (kJ mol^{-1}) solid reference (this work)
1273	74.4 ± 0.8	-98.0 ± 1.1	-101.9	-81.7 ± 1.1
1373	72.0 ± 1.0	-94.6 ± 1.4	-98.9	-80.8 ± 1.4
1473	68.8 ± 0.8	-90.0 ± 1.1	-96.0	-78.7 ± 1.1
1573	64.8 ± 0.8	-84.5 ± 1.1	-93.1	-75.6 ± 1.1
1673	60.0 ± 1.0	-78.4 ± 1.1	-90.1	-72.0 ± 1.1
1773	54.4 ± 0.8	-72.2 ± 0.8	-87.2	-68.3 ± 0.8
1873	47.2 ± 0.8	-66.0 ± 0.6	-84.2	-62.6 ± 0.6

Table 6. Comparison of our $\Delta_f G^0(Fe_2Zr)$ data with literature data.

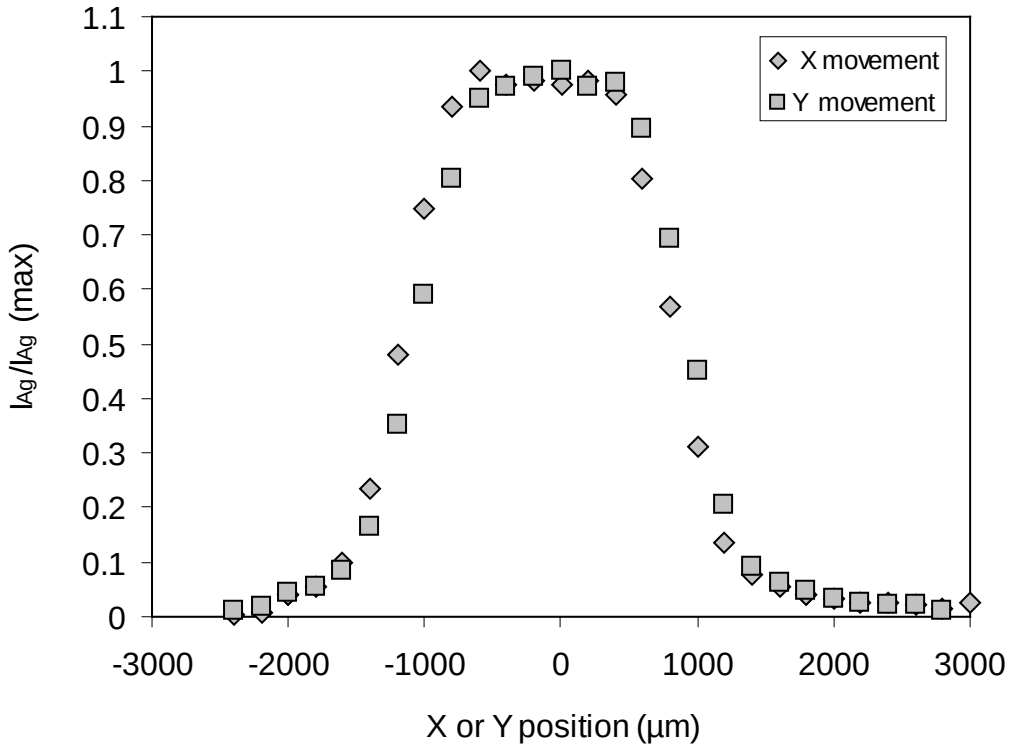

Figure 1. Normalized registration of Fe ion during X and Y movements of the effusion orifice for a cell containing pure iron sample at about 1739 K.

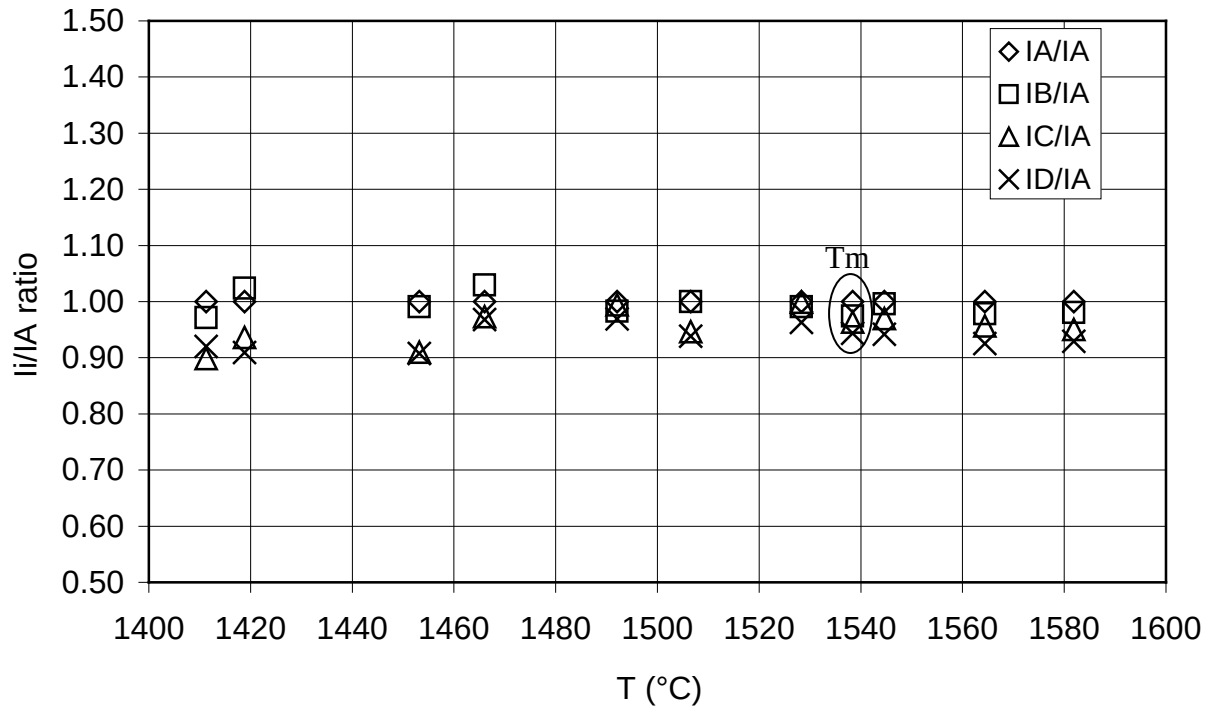

Figure 2. Ion intensity ratio of iron in each effusion cell as function of the measured temperature.

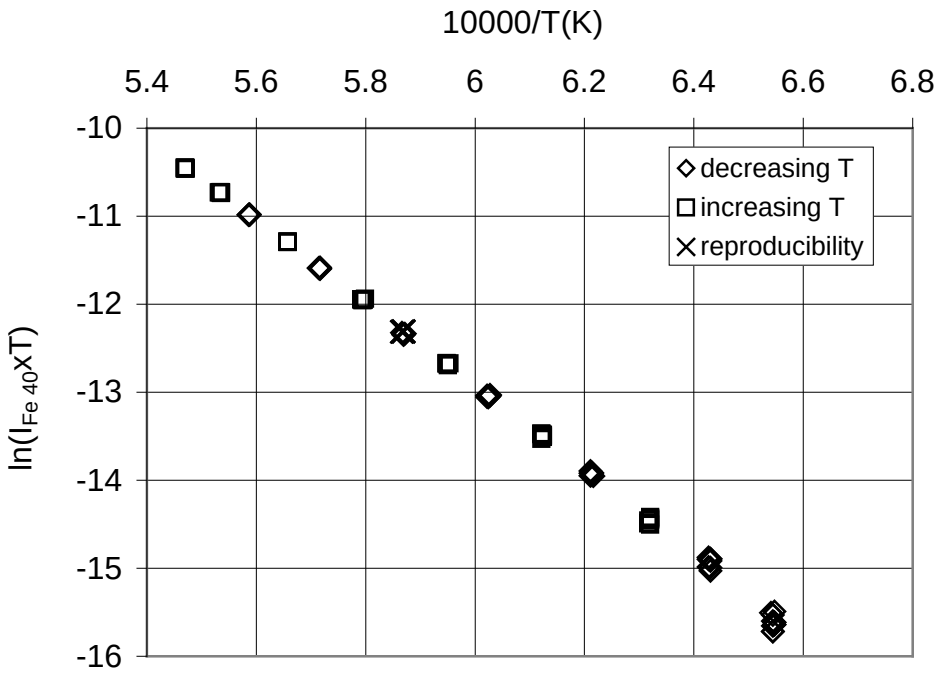

Figure 3. Iron intensity in Fe40Zr60 alloy versus measured temperature

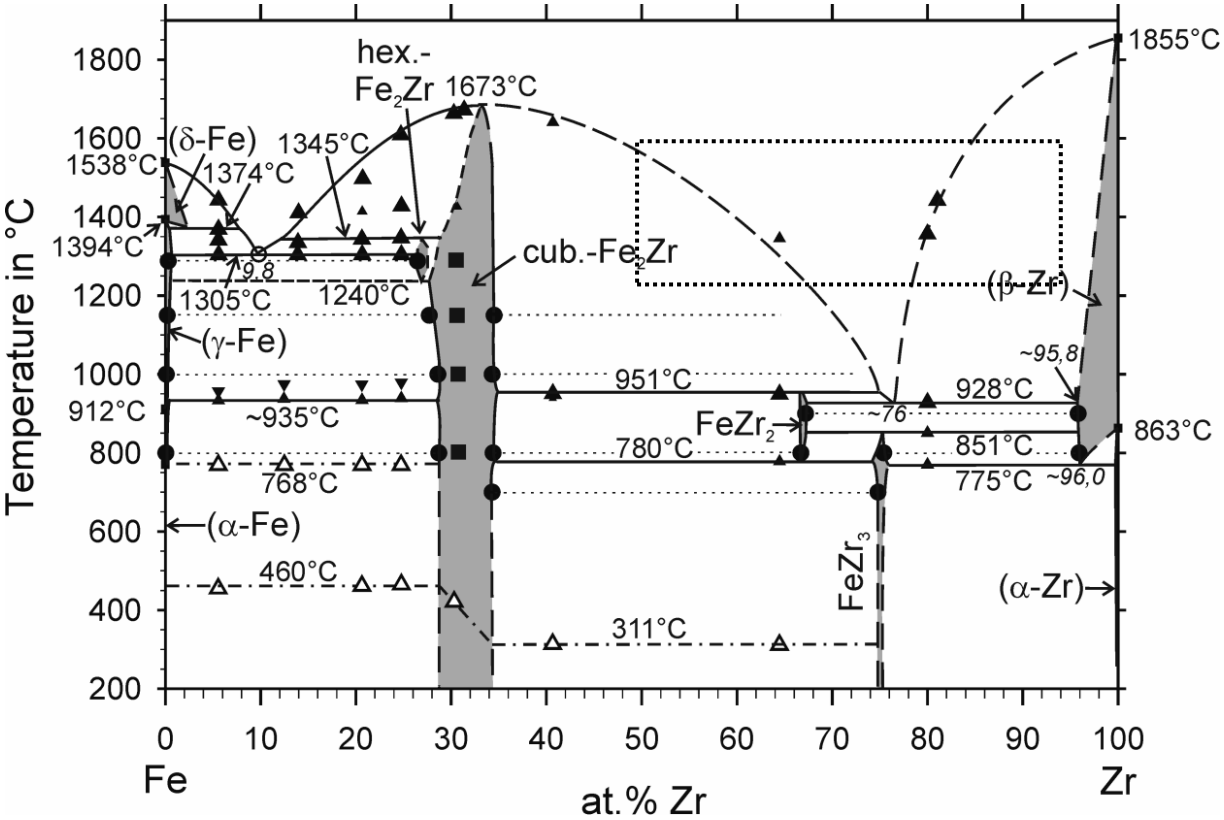

Figure 4. Experimental Fe-Zr phase diagram proposed by Stein [10] according his experimental results and our investigated area (dashed area) by mass spectrometry.

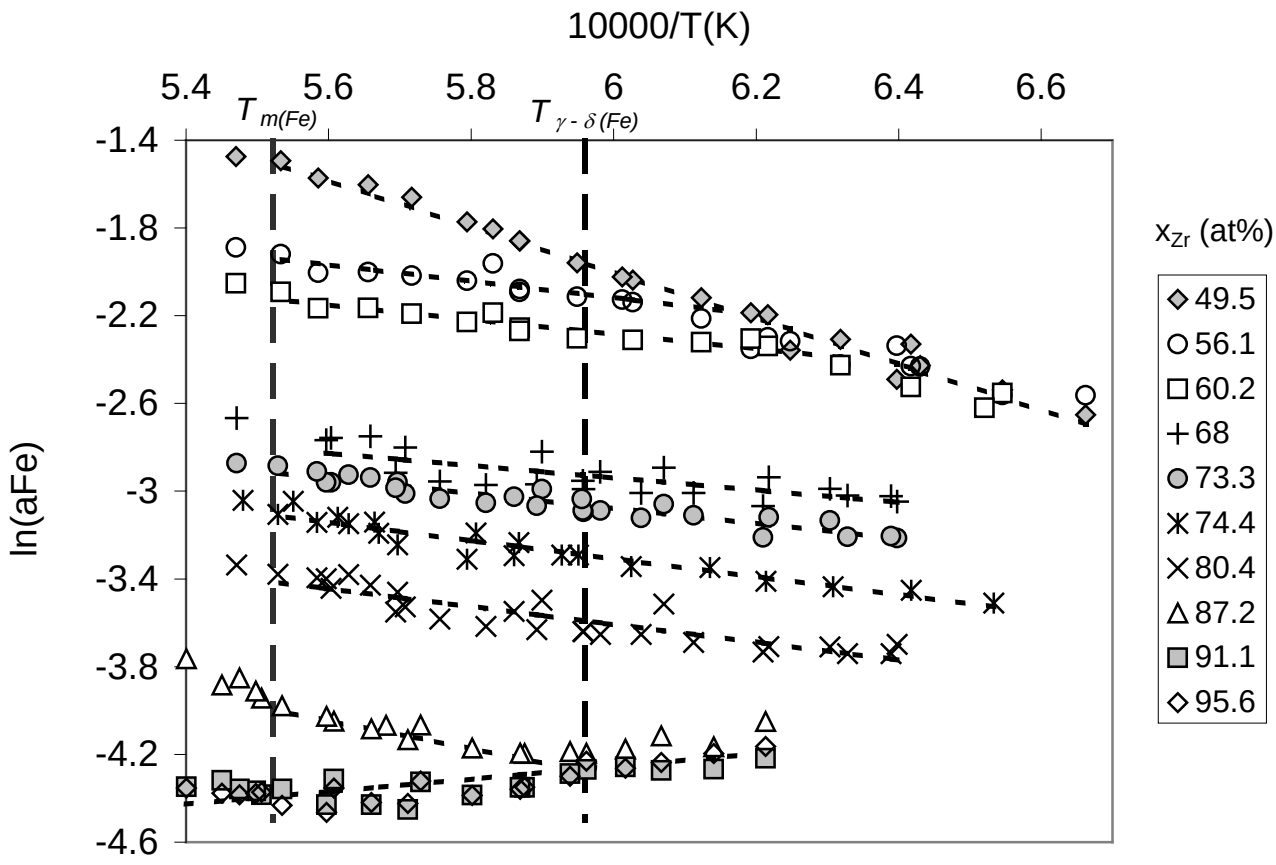

Figure 5. Natural logarithm of our experimental iron activity data in different Fe-Zr alloys.

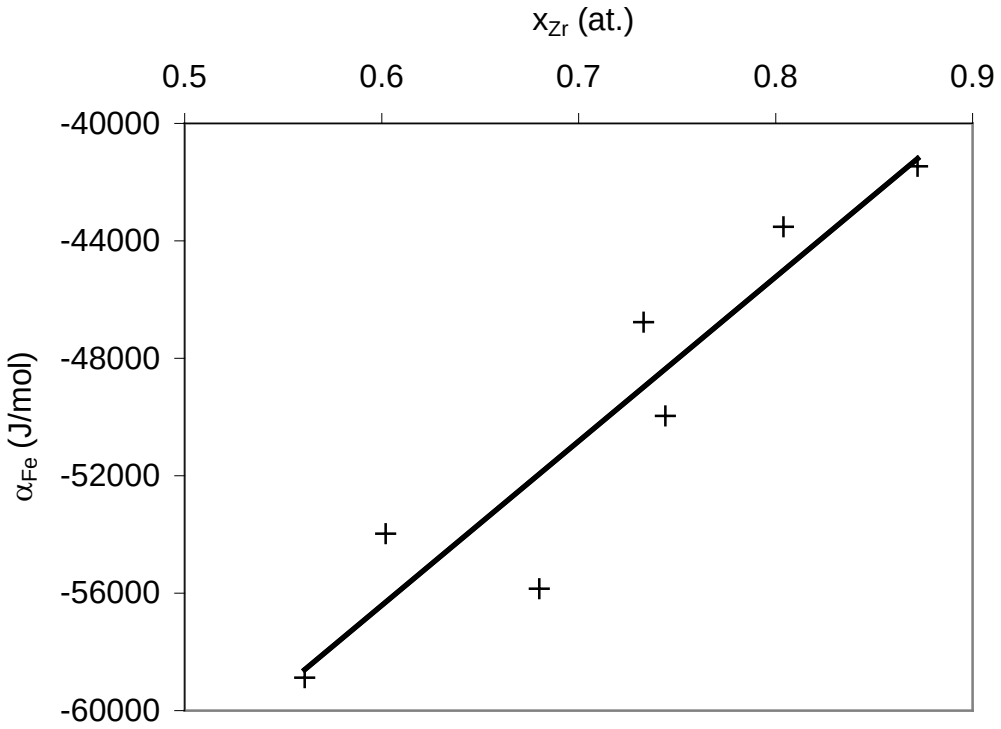

Figure 6. The function $\alpha_{Fe} = f(x_{Zr})$ at T = 1700 K

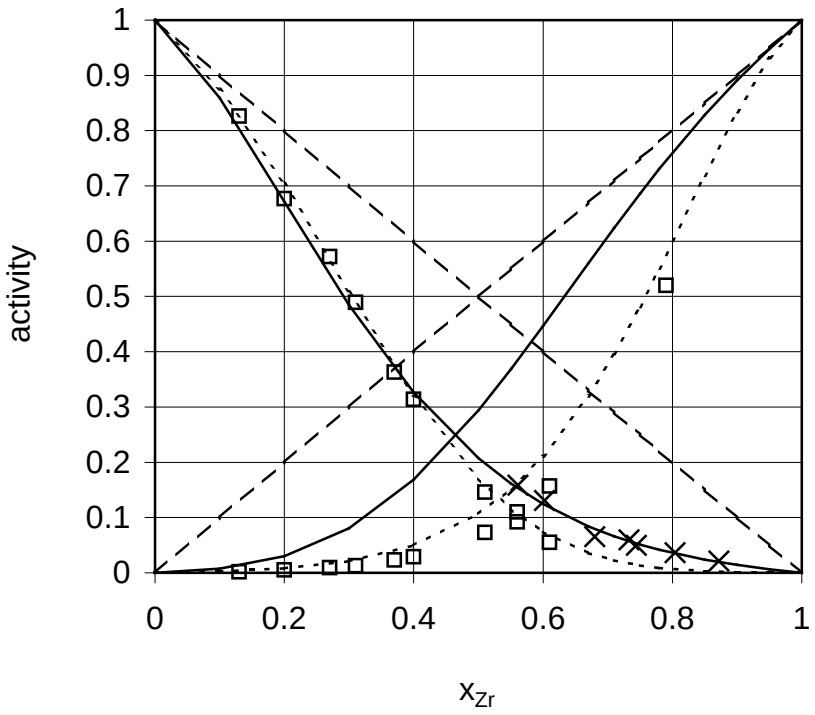

Figure 7. Comparison of our activity measurements referred to pure liquid elements with those deduced from literature at 1873 K; × : our experimental a_{Fe}, — : activities deduced from our equations (4) and (6), - - - : Pelton's results calculated from equation (8), □ : Schindlorova's and al. calculated values [14].

[1] Dupin N, Ansara I, Servant C, Toffolon C, Lemaignan C, Brachet JC. A thermodynamic database for zirconium alloys. J. Nucl. Mater. 1999;275:287-295.

[2] Guéneau C, Dauvois V, Pérodeaud P, Gonella C, Dugne O. Liquid immiscibility in a (O,U,Zr) model corium, J. Nucl. Mater. 1998;254:158-174.

[3] Arias D and Abriata JP. The Fe-Zr system. Bull Alloy Phase Diagrams. 1988;9:597-604

[4] Arias D, Granovsky MS and Abriata JP. Phase Diagrams of Binary Iron Alloys, ASM International, Materials Park, OH, 1993, p.467-472

[5] Alekseeva ZM and Korotkova NV. Izv. Akd. Nauk SSSR, Metall. 1989;4:202-208

[6] Okamoto H. Fe-Zr. J. Phase Equilibria. 1993;14:652-653

[7] Pelton AD. Thermodynamic analysis of phase equilibria in the iron-zirconium system. J. Nucl. Mater. 1993;201:218-224

[8] Servant C, Guéneau C, Ansara I. Experimental and thermodynamic assessment of the Fe-Zr system. J. Alloys Compounds. 1995;220:19-26

[9] Jiang m, Oikawa K, Ikeshoji T, Wulff L, and Ishida K. Thermodynamic Calculations of the Fe-Zr and Fe-Zr-C Systems. J. Phase Equilibria. 2001;22:406-417.

[10] Stein F, Dauthoff G, and Palm M. Experimental Determination of Intermetallic Phases, Phase Equilibria, and Invariant Reaction Temperatures in the Fe-Zr System. J. Phase Equilibria. 2002;23:480-494

[11] Sudavtsova VS, Kurach VP and Batalin GI. Thermochemical, properties of liquid binary alloys Fe-(Y, Zr, Nb, Mo). Izv. Akad. Nauk SSSR, Metall. 1987;3:60-61

[12] Sidorov OYu, Valishev MG, Esin YuO and Gel'd PV. Formation heat of iron-zirconium melts. Izv. Akad. Nauk SSSR, Metall. 1988;6:23-25

[13] Wang H, Lück R and Predel B. Kalorimetrische Bestimmung der Mischungsenthalpien flüssiger Eisen-Zirkonium-Legierungen. Z. Metallkd. 1990 ;81 :843-846

[14] Schindlorova V and Buzek Z, Sbornik Vedeckych Praci VSB. 1967 ;C.2/3 :157

[15] Svechnikov VN, Pan VM and SpectorAT. Russ. J. Inorg. Chem. 1963;8:1106

[16] Chatillon C, Pattoret A and Drowart J. Etudes thermodynamiques des phases condensées par spectrométrie de masse à haute température : Analyse de la méthode et revue des résultats. High Temp.-High Pressures. 1975;7:119-148.

[17] Kato E., J. Mass Spectrom. Soc. Jpn. 1993; 41,297-316

[18] Chatain S, Gonella C, Bordier G, Le Ny J. Thermodynamic activity measurements of the liquid Cu-Gd alloy by high temperature mass spectrometry. J. Alloys Compounds. 1995;228:112-118.

[19] Gardie P, Bordier G, Poupeau JJ and Le Ny J. Thermodynamic activity measurements of U-Fe and U-GA alloys by mass spectrometry. J. Nucl. Mater. 1992;189:85-96

[20] Baïchi M, Chatillon C, Guéneau C, Chatain S. Mass spectrometry study of UO_2-ZrO_2 pseudo-binary system. J. Nucl. Mater. 2001;294:84-87.

[21] Chatain S, Guéneau C, Chatillon C. High temperature mass spectrometry : Application to the thermodynamic study of Fe-Zr system, J. Nucl. Mater. 2005 ; 281-284.

[22] Alcock CB, Itkin VP and Horrigan MK. Vapor Pressure Equations of the Metallic Elements 298-2000 K, Department of Metallurgy and Materials Science, University of Toronto.

[23] Hultgren R, Desai PD, Hawkins DT, Gleiser M, Kelley KK and Wagman DD. Selected Values of the Thermodynamic Properties of the Elements. ASM Metals Park, 1973, p. 181.

[24] Paule RC.and Mandel J. Analysis of interlaboratory measurements on the vapor pressure of gold. Pure Appl. Chem. 1972;31:371-394

[25] Pankratz LB., Thermodynamic Properties of Elements and Oxides (United States Department of Interior, Bureau of Mines, 1982)

[26] Darken LS and Gurry RW, Physical Chemistry of Metals (McGraw-Hills, New-York, 1953) p.264

[27] Chase Jr MW, Davies JR, Downey JR, Frurip DJ, McDonald RA and Syverud AN., JANAF Thermochemical Tables 3rd ed. (National Bureau of Standards, Washington, 1986)

[28] Gachon JC and Hertz J. Thermodynamic analysis of phase equilibria in the iron-zirconium system. Calphad. 1983;7:1-12